Wave-current interaction over bedforms: observations and model predictions

Huw, J. POWELL[1,3]; George, VOULGARIS[1,4]; Michael, B. COLLINS[1] and Alex, C. BASTOS[1]

[1] School of Ocean and Earth Sciences, University of Southampton, Southampton Oceanography Centre, UK Fax.: (44) 1703 593059
Email: acb4@soc.soton.ac.uk
[2]Hydraulics Research, Wallingford, Oxforshire, OX10 8BA, UK
Email: rls@hrwallingford.co.uk
[3] now at CEFAS, Pakefield Road, Lowestoft, Suffolk, NR33 0HT, UK Fax (0)1502 524569
Email: h.j.powell@cefas.co.uk
[4] now University of South Carolina, Dept. of Geological Sciences, Columbia SC29208, USA
Email: gvoulgaris@sc.edu

Abstract
Hydrodynamic data collected under the combined action of waves and currents are combined with sea bed observations, in order to investigate sea bed roughness and sediment transport. Six bottom roughness models are tested using field data from the southern North Sea. The results indicate that the model of Nielsen (1983) most closely predicts the bottom roughness encountered due to the presence of ripples on a sandy bed. A refined model is proposed that combines the widely-held dependence upon bedform height, and a dependence upon the angle made between the tidal current direction and the bedform crest orientation:

$$\log(k_s) = 4.09h\cos q_{cr} - 3.42$$

Introduction
The formation and disappearance of sediment bedforms occurring under the action of waves and currents is the result of a complex interaction between the fluid and the underlying sediment; this is poorly understood, yet extremely important, in both physical and numerical models of coastal processes. Bedforms affect bottom roughness and shear stresses, wave attenuation, and sediment transport. Improved predictors for bedform geometry will lead naturally to better models of coastal processes, involving the movement of sediments.

The boundary shear stress depends upon sea bed roughness (k_s); this consists of 2 components, due to individual sand grains (skin friction) and the presence of bedforms (form drag). The roughness related to the bedforms is specified usually as a function of the bedform height (η) and steepness (η/λ) (Shinohara and Tsubaki, 1959; Nielsen, 1983; Xu and Wright, 1995; van Rijn, 1982, Grant and Madsen, 1982; Raudkivi, 1990, Drake et al., 1992).

The present investigation matches mean observed bed shear stresses (HR, 1991) with predicted (modelled) shear stresses, by adjusting model input parameters: the relationship between bed roughnes; bedform geometry; and measured instantaneous current velocities. Using the roughness derived in this investigation, Powell et al. (this volume) determines total bed shear stresses which are then reduced to allow for the form drag component of shear stress. These investigators predict sediment transport rates utilising 10 established formulae and compare their predictions with sediment transport rates derived independently from ripple migration rates.

1. Field Site and Data Collection
Hydrodynamic data and sea bed observations were obtained in the vicinity of well-developed sand banks off the Norfolk coast, UK, during November 1988. The mean water depth was approximately 29 m and the bed sediment consisted of well sorted sand, with a mean grain size of approximately 0.22 mm. An autonomous multi-sensor tripod, STABLE (Sediment Transport And Boundary Layer Equipment, Humphery, 1987), was used for this purpose. STABLE is capable of measuring simultaneous hydrodynamic conditions due to waves and currents, and the resulting response of the sea bed substrate. The STABLE instrument suite consists of 2 orthogonally-arranged pairs of annular electromagnetic current meters, at heights of 41 and 80 cm above the bed; these were used to record the 3 components of current velocity. A pressure sensor was used to provide estimates of mean water depth. The instruments were sampled, in 'burst' mode, at 4 Hz for a period of 512 s. Burst data were recorded at 2 hr intervals. Sea bed observations were obtained using a 35 mm camera, located at 1.25 m above the bed and looking vertically downwards. The sea bed was illuminated obliquely by a flashlight, angled approximately 44° from the horizontal. Shadows were cast on the sea bed by two graduated bars, positioned in the path of the flash light at 0.25 and 0.325 m above the sea bed.The STABLE bed frame was deployed on the

southwestern side of Broken Bank (Figure 1) for a period of approximately 3 days. Additional deployment and data collection details are presented by Collins (1991) and HR (1991).

2. Methods of Data Analysis

Hydrodynamics

Instantaneous horizontal currents (u,v) were measured at heights of 41 cm and 80 cm above the sea bed. The mean tidal speed at each height was calculated, by the vector addition of the orthogonal components. Equivalent parameters for the wave orbital motions have been derived similarly. Observed bed shear stresses have been determined for each burst, from several independent approaches (HR, 1991); estimates were made based upon the magnitude of the Reynolds stresses at both elevations, and upon the turbulent kinetic energy at both elevations. A further estimate was determined based upon the average of these 4 values. Estimates based upon the turbulent kinetic energy (E) at 0.8m above the bed, were found to be in closest agreement with the recorded flow data; as such, there have been selected to represent the stresses active on the sea bed, for the remainder of the present investigation. E is determined by:

$$E = \frac{1}{2}\left(\overline{u_t^2} + \overline{v_t^2} + \overline{w_t^2}\right) \quad (1)$$

where u_t, v_t and w_t are the turbulence variances in the x, y and z directions, respectively, at 80 cm above the sea bed. The mean bed shear stress (τ_c) is determined by:

$$t_c = arE \quad (2)$$

where a is a constant of proportionality, equal to 0.19, observed in a wide variety of flows (Soulsby, 1983).
The wave shear stress (τ_w) has been obtained using recorded wave characteristics and the boundary layer model (Sleath, 1991) for each burst.

Ripple geometry

Ripple dimensions were derived from the sea bed photographs, using a method described earlier by Sternberg (1967) and Kachel and Sternberg (1971). Sea bed topography has been investigated by casting the shadow of a solid straight bar onto the sea bed. Distortion of the shadow from a straight, true representation of the bar is due then to local sea bed topography. The distorted shadow can be observed and photographed. The (known) geometrical positions of the camera, flashlight and shadow bars can be used to determine the local sea bed topography from the trace of the shadow. Ripple heights and wavelengths are determined from the photographs using a method similar to that described by Wilkinson *et al.* (1985).

Bed roughness analysis

An iterative technique, using Sleath's (1991) model and the recorded hydrodynamic data, has been used to determine the roughness parameter for each burst. The roughness parameter is adjusted within the model, so that the mean shear stress predicted by the model matches the observed shear stress. The relationship between the roughness values obtained in this way has been compared with the recorded hydrodynamic data and sea bed observations.

3. Results

27 burst data sets were collected with a photograph of the sea bed obtained at the beginning and end of each burst (Table 1). During the deployment, tidal current speeds ranged from approximately 20 cm s^{-1} to 90 cm s^{-1}, whilst the root-mean squared (rms) orbital velocities ranged from approximately 10 cm s^{-1} to 24 cm s^{-1}. The average wave period was 10.3 s. The transverse velocity component was consistently the dominant flow component, at both elevations. Hence, the flow velocities throughout the experiment were largely unobstructed by STABLE.

Wave activity

Wave orbital velocities recorded at 0.8m above the bed (u_{b80}) have been compared with those recorded concurrently at 0.41m (u_{b41}). The regression line has a slope of 1.22, and the orbital velocities exhibit a correlation coefficient of 0.99. Linear wave theory suggests that the difference between orbital velocities at these elevations above the bed should be very small, hence the slope of the line should be almost unity. The STABLE data indicate that u_{b80} is consistently greater than u_{b41}, the difference increasing with wave activity. Soulsby and Humphery (1990) have presented elsewhere wave orbital velocities (u_{b40}, u_{b10}) recorded over a flat featureless

mixture of gravel, sand and shell. These investigators found also that the slope of the regression line was 1.22, with a correlation coefficient of 0.96. In common with the present data, the deviation from the line of equality increases with increasing wave activity.

To explain the difference in orbital velocity with height, further field data is required to resolve the oscillatory flow closer to the bed. Possible explanations of increasing orbital velocity with height must come from theoretical considerations of wave-current interactions (although no mathematical model has been used to simulate the results). It is possible that first order wave theory, used by most wave-current interaction models, may not be an accurate representation of the orbital velocities at this location. Hence, it would appear that further investigation is required.

Bedforms

Sea bed photographs corresponding to 15 sampling 'bursts' were of high quality and showed clear images of the rippled seabed, which were capable of being analysed. The highest number of ripples observed in any one photograph was 4. Typically this value was 2 providing multiple estimates of ripple dimensions present during that burst. Ripple profiles were predominantly asymmetric, with heights of between 0.4 and 2 cm (average 1 cm), and wavelengths of between 11 and 22 cm (average 15 cm). The height and spacing characteristics of the ripples observed on the sea bed were investigated.

The results obtained here have been compared with those obtained by Amos *et al*. (1988) and by Miller and Komar (1980). Miller and Komar (*op. cit*.) investigated laboratory data on the geometry of oscillation ripples, collected by a number of investigators using a variety of experimental devices. Miller and Komar found that a linear relationship existed between the wave orbital diameter (d_0) and the ripple spacing, λ (equivalent to the ripple wavelength):

$$l = 0.65 d_0 \tag{3}$$

The results show that the average conditions experienced during the STABLE deployment, plot in the region of the relationship suggested by Miller and Komar when the wave orbital diameter was determined using the root-mean-square wave height. The STABLE data plot very close to the data observed by Amos *et al*. (*op. cit*.). These investigators used an autonomous, free-standing tripod (*Ralph*), deployed in 22 m of water over a well-sorted sandy bed on the Canadian continental shelf. As such, this site is very similar to the deployment site of STABLE. Similar wave characteristics were observed during these 2 deployments. However, significantly weaker tidal currents were observed during the *Ralph* deployment.

The present data, together with those of Amos *et al*. (1988), are in close agreement with the empirical relationship suggested by Miller and Komar (*op. cit*.) between grain diameter and ripple spacing:

$$l = 0.0028 D^{1.68} \tag{4}$$

where the grain diameter (D) is given in microns, and the ripple spacing (λ) is in centimetres. The ripples observed during the present investigation are in agreement with the relationship suggested by Yalin (1977):

$$l = bD \tag{5}$$

Yalin suggests that b=0.1; for the present investigation b=0.07.

The bedform geometry obtained here has been compared with results from previous investigations. Ripples have been shown to develop during times when the bed material is moving primarily as bedload (Wiberg and Harris, 1994). The geometry of sea bed ripples depends significantly on the prevailing sediment transport conditions. From this discussion it can be seen that the bedform geometry obtained from the STABLE deployment exhibits characteristics associated with both wave- and current-dominated ripples. However, the ripples were observed under current-dominated conditions and were observed to be asymmetrical; this is a feature not associated with ripples generated in pure oscillatory flows. However, from the agreement with previous investigations into wave generated ripples, it would appear that the wave conditions present during the STABLE deployment may have some influence on bedform geometry. The super-position of a mean current on an oscillatory flow can add a degree of asymmetry to the ripples in the direction of the mean flow; asymmetry in orbital velocities can also cause ripple asymmetry (Clifton and Dingler, 1984).

The accuracy of the bedform size values must be considered. The photographs were digitised by eye and, therefore, were somewhat subjective. Some bursts contained significant amounts of suspended sediment; therefore, these photographs could not be used to determine bedform dimensions. Hence the dimensions observed here are those which were evident under lower flow conditions.

Bed roughness

The roughness derived from matching the 'observed' stresses with those obtained from the boundary layer model, has been examined in light of other recorded data. Values of the roughness parameter (k_s) were found to be dependent upon the height of the roughness elements and, similar to the relationship suggested by Drake *et al.* (1992), the angle between the ripple crests and the steady current direction (Figure 2). This relationship can be represented by:

$$\log(k_s) = K_1 h \cos q_{cr} - K_2 \qquad (6)$$

The values of K_1 and K_2, based on a line of 'best fit' through the data, were found to be 4.09 and 3.42, respectively. These are, in effect, measured values of bed roughness. These 'measured' roughness values can be compared with the values obtained from the 6 formulae described earlier. The ratio of predicted to measured values has been evaluated in terms of an error parameter P, which is given by:

$$P = \frac{k_s(predicted)}{k_s(measured)} \qquad (7)$$

The results of this investigation into predicted bed roughness values are presented in Table 2. The wide range of values of P associated with the investigation can be seen. Those equations with P values closest to unity have most accurately reproduced the observed roughness values. Three bands of accuracy were investigated: $1/2 \le P \le 2$, $1/3 \le P \le 3$ and $1/5 \le P \le 5$.

Of the formulae investigated here, 3 provide roughness estimates similar to those obtained by comparing the Reynolds stresses with those obtained using the model of Christoffersen and Jonsson (1985). Whilst the roughness values predicted by the formulae of van Rijn (1982), Nielsen (1983) and Raudkivi (1990) were, on average, 1.25, 0.87 and 1.36 times the 'measured' values, respectively, there is considerable scatter about these mean values. The better performance of the Nielsen model, although only slight here, is found also for moderate conditions by Xu and Wright (1995). The formulae of Shinohara and Tsubaki (1959) and Grant and Madsen (1982), however, provided a greater number of roughness estimates within the widest tolerance band. Drake *et al.*'s (1992) modification of Grant and Madsen's (1982) formula, when applied to the observations obtained here, produced values which were inconsistent with those 'measured'. In the present investigation, θ_{cr} varied between 18° and 57°; this is a range similar to that experienced by Drake *et al.* (5° to 46°). However, these investigators experienced relatively low currents and waves and, therefore, an absence of any significant bed erosion and resuspension (Drake *et al.*, 1992).

4. Conclusion

Sea bed geometry can be interpreted successfully from time-lapse photography. The time delay between photos at either 'end' of a burst, 17 minutes, can be too great to allow ripples to be identified convincingly on both of the photographs. Therefore, during the stages of higher flow, migration rates can be more difficult to quantify. In order that the problems associated with ripple aliasing are minimised, sampling intervals of shorter duration are required. However, considerable uncertainties exist in the methods of determining ripple dimensions and inferring sediment transport rates.

Existing formulae for describing the sea bed roughness, due to the presence of bedforms, can produce significantly differing results. The physical roughness encountered in this investigation was found to be represented most accurately by Nielsen's (1983) formula. In the present investigation k_s was found, however, to be dependent upon the bedform height, and the angle between current direction and ripple crests; a new formula is suggested (Equation 6).

References

Amos, CL, Bowen AJ, Huntley, DA and Lewis, CFM, 1988. Ripple generation under the combined influences of waves and currents on the Canadian continental shelf. *Continental Shelf Research*, **8**(10), 1129-1153.

Christoffersen, JB and Jonsson, IG, 1985. Bed friction and dissipation in a combined current and wave motion. *Ocean Engineering*, **12**(5), 387-423.

Clifton, HE and Dingler, JR, 1984. Wave-formed structures and paleoenvironmental reconstruction. Developments in Sedimentology, 39. Greenwood B and Davies Jr. RA (Eds). Elsevier Science Publishers, 165-198.

Collins, MB, 1991. RRS Challenger Cruise 40, 15-29 November 1988. Sediment and water movement in the vicinity of a North Sea sandbank. Southampton: Southampton University, Department of Oceanography. 38pp.

Drake, DE, Cacchione, DA and Grant, WD, 1992. Shear stress and bed roughness estimates for combined wave and current flows over a rippled bed. *Journal of Geophysical Research*, **97**(C2), 2319-2326.

Grant, WD and Madsen, OS, 1982. Moveable bed roughness in unsteady oscillatory flow. *Journal of Geophysical Research*, **87**(C1), 469-481.

HR, 1991. Norfolk Sand Banks, Analysis of STABLE data. Hydraulics Research, Wallingford, Report EX 2345, 18pp.

Humphery, JD, 1987. STABLE- an instrument for studying current structure and sediment transport in the benthic boundary layer. Proc. Electronics for Ocean Technology Conf. Endinburgh.

Kachel, NB and Sternberg, RW, 1971. Transport of bedload as ripples during an ebb current. *Marine Geology*, **10**, 229-244.

Miller, MC and Komar, PD, 1980. Oscillation sand ripples generated by laboratory apparatus. *Journal of Sedimentary Petrology*, **50**(1), 173-182.

Nielsen, P, 1983. Analytical determination of nearshore wave height variation due to refraction shoaling and friction. *Coastal Engineering*, **7**, 233-251.

Powell, HJ, Voulgaris, G, Collins, MB, Bastos, AC, Soulsby, RL, 2000. Sediment transport rates over bedforms: Observations and model predictions. *In this volume.*

Raudkivi, AJ, 1990. Loose boundary hydraulics. 3rd ed, Pergammon Press, 533pp.

Shinohara, K and Tsubaki, T, 1959. On the characteristics of sand waves formed upon beds of open channels and rivers. Reports of Research Institute for Applied Mechanics, Kyushu University, Japan, 7, No. 25.

Sleath, JFA, 1991. Velocities and shear stresses in wave-current flows. *Journal of Geophysical Research*, **96**(C8), 15237-15244.

Soulsby, RL, 1983. The bottom boundary layer of shelf seas. In: Physical Oceanography of Coastal and Shelf Seas. Johns B (Ed). Elsevier Oceanography Series 35, Elsevier, Amsterdam, 189-266.

Soulsby, RL and Humphery, JD, 1990. Field observations of wave-current interaction at the sea bed. In: Proc Advanced Workshop on Water Wave Linematics, Torum A (Ed), Molde, Norway. Kluner.

Sternberg, RW, 1967. Measurements of sediment movement and ripple migration in a shallow marine environment. *Marine Geology*, **5**, 195-205.

van Rijn, LC, 1982. Equivalent roughness of an alluvial bed. *Journal of the Hydraulics Division*, ASCE, **108**, 1215-1218.

Wiberg, PL and Harris, CK, 1994. Ripple geometry in wave-dominated environments. *Journal of Geophysical Research*, **99**(C1), 775-789.

Wilkinson, RH, Moore, EJ and Salkield, AP, 1985. Photogrammetry in sediment transport studies. In: Underwater Photography and Television for Scientists, George JD, Lythgoe GI and Lythgoe JN (Eds), Underwater Assoc. Spec. Vol., 2. Clarendon, 13pp.

Xu, JP and Wright, LD, 1995. Tests of bed roughness models using field data from the Middle Atlantic Bight. *Continental Shelf Research*, **15**, 1409-1434.

Yalin, MS, 1977. On the determination of ripple length. ASCE, HY4, 439-442.

Burst	Waterd epth (m)	Wave period (s)	Wave orbital velocity (cm s^{-1}) 41 cm 80 cm	Wave-current interaction angle (°)	Current velocity (cm s^{-1}) 41 cm 80 cm
1	28.50	9.11	17.27, 20.96	48.7	48.60, 55.83
2	29.20	9.50	15.93, 19.15	25.7	60.98, 80.80
3	29.06	9.09	15.78, 18.89	5.4	28.39, 37.45
4	29.64	10.60	15.20, 18.40	57.6	17.10, 20.10
5	29.41	11.01	11.85, 13.83	33.4	45.04, 57.58
6	28.67	10.63	13.24, 15.33	22.1	24.36, 31.89
7	28.04	10.25	10.90, 13.09	39.7	21.09, 29.44
8	28.23	10.53	13.87, 16.60	26.0	48.02, 65.67
9	28.85	10.65	12.72, 15.57	9.3	22.04, 30.53
10	29.69	10.72	12.47, 14.70	39.1	32.11, 43.27
11	29.81	10.79	10.82, 13.15	35.1	61.35, 80.51
12	29.41	10.97	13.28, 16.00	24.0	51.68, 68.32
13	28.43	10.86	14.86, 17.96	78.7	12.97, 11.92
14	28.25	8.64	15.94, 19.90	27.4	59.69, 81.84
15	28.59	10.74	16.40, 19.57	16.2	55.70, 78.61
16	29.28	10.90	18.34, 22.40	77.3	7.70, 11.94
17	29.59	10.06	15.10, 17.56	42.4	41.11, 55.80
18	29.06	8.63	15.81, 18.97	29.0	43.75, 59.04
19	28.08	9.96	14.62, 17.80	79.9	15.10, 18.19
20	27.91	8.46	17.00, 20.75	15.8	59.88, 82.07
21	28.36	9.87	19.78, 23.89	19.0	45.75, 64.11
22	29.28	11.10	19.96, 23.99	63.8	11.08, 15.70
23	29.99	12.09	16.70, 19.30	38.2	47.16, 63.44
24	29.85	10.99	15.98, 18.47	30.7	66.01, 88.82
25	29.04	11.07	15.27, 17.56	5.8	25.98, 40.32
26	28.18	10.60	16.56, 19.89	45.0	40.45, 52.39
27	28.47	11.32	17.17, 20.31	19.2	66.44, 90.90

Table 1 'Burst-averaged' hydrodynamic data recorded during the deployment.
Note: Bursts were approximately 17 mins long, recorded once every 2 hours. Burst 1 was recorded from 1403 hrs on 19/11/88.

Burst	**Observed roughness (m)**	**Ratio of predicted roughness to observed roughness (P)**					
		GM82	Nielsen (1983)	Drake *et al.* (1992)	Raudkivi (1990)	ST59	van Rijn (1982)
2	0.029	0.93	0.28	-89.11	0.43	0.81	0.45
4	0.400	0.04	0.00	-17.62	0.02	0.03	0.02
5	0.046	0.29	0.09	-100.03	0.14	0.28	0.16
7	0.118	0.25	0.08	-28.53	0.11	0.20	0.11
8	0.011	1.62	0.46	-318.44	0.76	1.41	0.79
9	0.050	0.48	0.14	-55.33	0.22	0.36	0.19
10	0.010	1.83	0.55	-307.02	0.85	1.57	0.87
14	0.004	1.93	0.64	-865.14	0.90	0.98	1.15
15	0.004	12.58	3.64	-431.41	5.86	9.06	4.49
16	0.400	0.03	0.01	-25.92	0.01	0.03	0.02
17	0.003	7.55	2.19	-782.75	3.51	6.39	3.52
18	0.003	9.39	3.00	-373.03	4.37	7.24	3.78
19	0.009	0.39	0.11	-957.34	0.18	0.47	0.27
20	0.002	2.95	0.82	-817.33	1.37	3.23	1.87
25	0.017	3.58	1.01	-96.69	1.67	2.34	1.06
P mean		2.92	0.87	-351.05	1.36	2.36	1.25
$0.5 \leq P \leq 2$		4	4	-	5	4	5
$0.3 \leq P \leq 3$		7	7	-	6	7	6
$0.2 \leq P \leq 5$		10	8	-	9	10	9

Table 2 The application of (six) predictive equations to reproduce the observed roughness values, expressed in terms of a P parameter (see text).
Key: GM82- Grant and Madsen (1982); ST59- Shinohara and Tsubaki (1959).

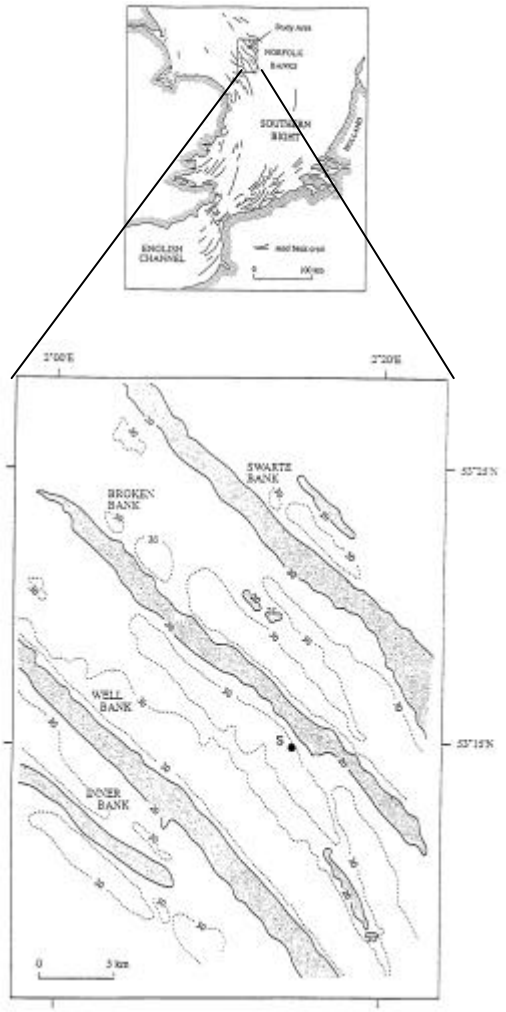

Figure 1 – Location of the present study area showing the position of STABLE deployment (S). Bathymetry in metres relative to Chart Datum.

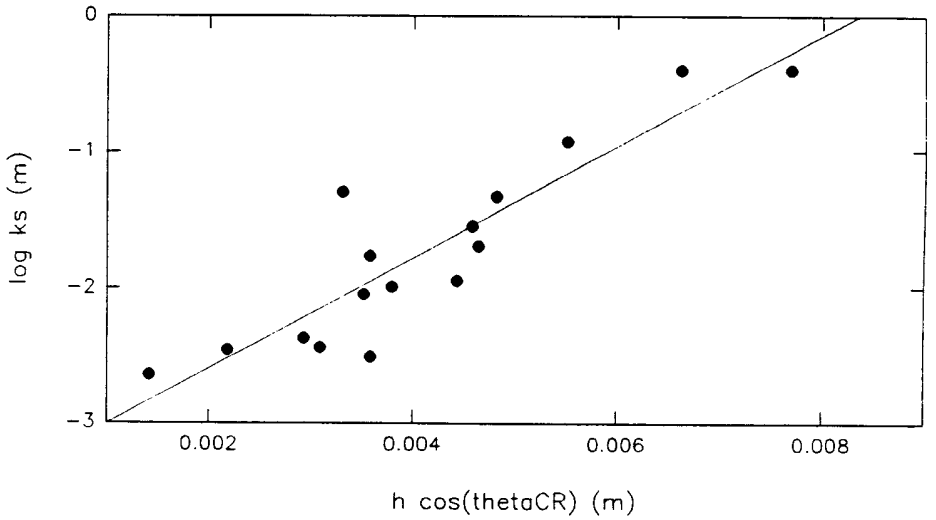

Figure 2 – Dependence of the bed roughness (k_s) upon the ripple height (h) and the angle made between the current direction and the ripple crests (thetaCR~θcr).